Title

Cold spot mapping inferred from MRI at time of failure predicts biopsy-proven local failure after permanent seed brachytherapy in prostate cancer patients: Implications for focal salvage brachytherapy

Journal

Radiotherapy and Oncology, 109(2)

ISSN

0167-8140

Authors

Crehange, Gilles
Krishnamurthy, Devan
Cunha, J Adam
et al.

Publication Date

2013-11-01

DOI

10.1016/j.radonc.2013.10.028

Peer reviewed

Published in final edited form as:
Radiother Oncol. 2013 November ; 109(2): 246–250. doi:10.1016/j.radonc.2013.10.028.

Cold spot mapping inferred from MRI at time of failure predicts biopsy-proven local failure after permanent seed brachytherapy in prostate cancer patients: Implications for focal salvage brachytherapy

Gilles Crehange[a,b,*], **Devan Krishnamurthy**[a], **J. Adam Cunha**[a], **Barby Pickett**[a], **John Kurhanewicz**[c], **I-Chow Hsu**[a], **Alexander R. Gottschalk**[a], **Katsuto Shinohara**[d], **Mack Roach III**[a,d], and **Jean Pouliot**[a]

[a]Department of Radiation Oncology, Helen Diller Family Comprehensive Cancer Center, UCSF, San Francisco, USA

[b]Department of Radiation Oncology, Dijon University Hospital, France

[c]Department of Radiology, University of California at San Francisco

[d]Department of Urology, Helen Diller Family Comprehensive Cancer Center, UCSF, San Francisco, USA

Abstract

1. To establish a method to evaluate dosimetry at the time of primary prostate permanent implant (pPPI) using MRI of the shrunken prostate at the time of failure (t_f).
2. To compare cold spot mapping with sextant-biopsy mapping at t_f.

Material and methods—Twenty-four patients were referred for biopsy-proven local failure (LF) after pPPI. Multiparametric MRI and combined-sextant biopsy with a central review of the pathology at t_f were systematically performed.

A model of the shrinking pattern was defined as a Volumetric Change Factor (VCF) as a function of time from time of pPPI (t_0). An isotropic expansion to both prostate volume (PV) and seed position (SP) coordinates determined at t_f was performed using a validated algorithm using the VCF.

Results—pPPI CT-based evaluation (at 4 weeks) vs. MR-based evaluation: Mean D90% was 145.23 ± 19.16 Gy [100.0–167.5] vs. 85.28 ± 27.36 Gy [39–139] (p = 0.001), respectively. Mean V100% was 91.6 ± 7.9% [70–100%] vs. 73.1 ± 13.8% [55–98%] (p = 0.0006), respectively. Seventy-seven per cent of the pathologically positive sextants were classified as cold.

*Corresponding author. Address: Department of Radiation Oncology, Helen Diller Family Comprehensive Cancer Center, 1600 Divisadero Street, San Francisco, CA 94143-1708, USA. gcrehange@cgfl.fr (G. Crehange).

Conflict of interest statement
None.

Conclusions—Patients with biopsy-proven LF had poorer implantation quality when evaluated by MRI several years after implantation. There is a strong relationship between microscopic involvement at t_f and cold spots.

Keywords

Prostate cancer; Prostate permanent implant; Seeds; Local failure; MR-based dosimetry

Prostate permanent implant with seeds (PPI) has become a valid therapeutic option with low morbidity, and the number of indications over the past decade has increased in both the United States and Europe [1]. Up to 30% of prostate cancer patients treated with PPI experience biochemical relapse during their follow-up [2,3]. Some have nodal or distant failure, which proves that their disease was systemic, while among patients with low-risk disease at baseline, those who fail are more likely to have exclusively intra-prostatic failure [4]. For patients with local failure (LF) only, what remains unclear is if the LF is located inside, at the edges of, or far from the volume that received the nominal dose.

Salvage brachytherapy has become feasible with promising results [5–8]. The identification of cold spots at time of failure ($t_{f)}$ could help to improve the dose distributions of the salvage plan and the quality of the salvage implantation while minimizing the volume of prostate and surrounding tissues irradiated.

We hypothesized that MR-based dose calculation several years after implantation could help to determine whether a tumor was related to a poor quality primary PPI (pPPI) (i.e. LF located inside the cold spots) or if it was more likely to be a radio-resistant tumor.

Materials and methods

Patient and treatment characteristics

Between June 1995 and January 2010, we identified 24 patients who were referred to the University of California San Francisco (UCSF) for an isolated biopsy-proven intra-prostatic failure after rising levels of PSA. The characteristics of the patients and tumors at the time of pPPI and tumor characteristics at t_f are presented in Table 1. Because of post-radiation effects, the Gleason score was unpredictable in seven patients reviewed by our pathologists at UCSF. Seventeen patients were treated with pPPI as monotherapy and seven patients as a boost to external beam radiotherapy.

MR imaging registration, delineation and seed reconstruction

Seeds were identified as any spot inside the prostate or the surrounding tissues with no signal. The slice thickness was small enough to make sure that seeds could not be missed. Each set of images was transferred from our PACS to our TPS dedicated for HDR-brachytherapy (OncentraMasterPlan, OMP v3.1 SP3, Nucletron®, Veenendal, Netherlands) (Fig. 1).

Each prostate was outlined by the same physician. Intra- and inter- observer variabilities in prostate contouring are far lower on MRI than on CT images [9–12]. The seminal vesicles at the base and the levator ani muscles at the apex were excluded, even if seeds were located

inside these areas. Then, as the number of seeds implanted for each patient was known it was possible to identify each seed on each slice by inserting the tip of a catheter at each seed (Fig. 1).

Reconstruction of the prostate volume at baseline

Calculating volume reduction between the prostate size at the time of pPPI (t_0) and t_f is an important issue that must be addressed in such an approach. An MRI-based volumetric analysis was performed on prostate cancer patients, who underwent PPI (without hormones or external beam) from 1996–2006. A model of the shrinking pattern was used to define a volumetric change factor (VCF) as a function of time from t_0 (Fig. 2). A deformation tool was designed to increase the size of the current MR images (with seed locations) so that an estimated isodose distribution at t_0 could be recalculated [13]. The deformation tool designed to accept the VCF was applied to the current MR images and an estimated isodose distribution at t_0 was generated.

For each patient, t_f was defined as the time between the date of the pPPI and the date of pathologically-proven LF. Thus, from the prostate volume at failure and the time to failure, it was possible to calculate prostate volume at baseline using the VCF calculated for each patient.

Reconstruction of initial seed location and inverse dosimetry

In order to calculate the correct dose distribution, it was necessary to recreate not only the original (larger) volume of the prostate but also the initial relative positions of the seeds. Isotropic prostate expansion was implemented using the center of mass of the contours as the isocenter of expansion (Fig. 3). This model was validated on a patient for whom MR images were available at both 30 days and t_f. The dose distribution was calculated using an in-house software following the TG-43 formalism. Isodose lines at 50% and 100% were generated on each slice and superimposed on the prostate contours.

Per-sextant comparisons

To determine any correlation between the cold sextants and the biopsy-proven invaded sextants, we decided to define a *cold sextant* as any sextant with a prostate contour outside the 100% IDL in every slice with less than 90% of the slice area covered by the 100% IDL (Fig. 4).

Statistics

Data are presented as numbers (percentages), or means (SD) and medians (Min–Max). All analyses were performed using Stata V11 software (StataCorp LP, College Station, TX). *p* Values were two-tailed and considered significant when no greater than 0.05. To assess the quality of the implant at t_0 and t_f, non-parametric Wilcoxon matched-pairs signed-ranks tests were performed.

Results

Seed identification and prostate volume

The mean number of seeds implanted at baseline was 84.1 [49– 146] with a mean number of seeds identified on MRI at t_f of 82.6 [49–143].

The mean interval between t_0 and t_f was 72.3 [18–145] months. Mean PV at t_f was 40.75 [21.8–71.8] cm^3. After applying VCF, we found a mean PV at t_0 of 63.66 [31.5–111.0] cm^3. Treatment characteristics are summarized in Table 1.

Comparison of dosimetric plans (baseline vs reconstructed)

D90% and V100% were significantly lower when evaluated several years after implantation: Mean D90% on post-PPI CT-based evaluation vs. MR-based evaluation at baseline were 145.23 ± 19.16 Gy [100.0–167.5 Gy] vs. 85.28 ± 27.36 Gy [39– 139 Gy] ($p = 0.001$). Mean V100% on post-PPI CT-based evaluation vs. MR-based evaluation at baseline were 91.55 ± 7.95% [70– 100%] vs. 73.10 ± 13.76% [55–98%] ($p = 0.0006$). Comparisons between D90% and V100% at t_0 vs. t_f are detailed in Table 2.

Topography of “cold spots”

Cold areas were more likely to be diffused cranio-caudally (apex: 75.0%, mid-gland: 0%, base: 62.5% and apex + base: 54.1%). The rates of anterior and posterior cold isodose areas were: 12.5% and 25.0% for the apex, 70.8% and 37.5% for the mid-gland, 20.8% and 16.6% for the base, respectively.

Correlation between cold spots and pathologically-invaded sextants

All but one of the patients had at least one pathologically-positive (*path+*) sextant that was cold, and 77% of *path+* sextants were classified as *cold*. Per patient, the mean number of *path+* sextants was 1.75 [1–5] whereas the mean number of “cold sextants” was 4.83 [0–6].

Discussion

After a very high dose of radiation such as after pPPI, an estimated 5–20% of low-intermediate risk patients and up to 50% of high-risk patients may experience biochemical failure [2,3,14]. Overall, nearly 8% of patients who undergo prostate brachytherapy harbor locally-persistent disease [15]. A biopsy-proven LF is more likely to be associated with a low dose of radiotherapy and is associated with a higher risk of death from prostate cancer [15]. In the context of curative salvage therapy, it is essential to determine whether these LFs could be caused by inadequate (i.e. too low) doses of radiation to some areas of the prostate as LF strongly increases the likelihood of late distant metastases over time [16].

In our study, we found that 75% of the patients were diffusely cold at the apex, 70.8% at the anterior part of mid-gland, 62.5% at the base and 54.1% at base + apex, with 77% of cold pathologically- positive sextants. These results raise questions as to whether this geographic miss could be due to a poor definition of the apex on US or CT axial slices or whether the area at the base and the apex could be too small to implant an adequate number of seeds in

the supero-inferior axis. Moreover, our biopsy-proven cancer detection rate could be underestimated since (6–10 cores) sextant biopsy is suboptimal. 3D mapping using a brachy template may explore the prostate, including lateral and anterior regions, more accurately.

In pPPI, even though the dose delivered is substantially higher than with external radiation, the geometry of the radioactive seeds leads to a dose distribution that can be very heterogeneous. This can create a higher likelihood of unintended low-dose areas, particularly if the seeds move within the prostate after implantation. For localized prostate cancer, a dose–response relationship has also been established with prostate brachytherapy [17]. Although the post-implant plan assessment may be unsure as it is associated with high inter-observer variability [18], the D90% remains the most significant predictor of biochemical failure (assuming the surrogacy for LF). Patients whose D90% is <140 Gy are more likely to experience biochemical failure (68% vs. 96%, $p = 0.0002$) while the rate of positive biopsies is significantly higher when D90% <160 Gy (22% vs. 9%) [19]. Although central and peripheral zones probably shrink differently after radiation therapy, zonal anatomy disappears on MRI several weeks after radiation. In our study, we hypothesized that seeds move along with the prostate in a homogeneous way, thus creating some unexpected low-dose areas in the follow-up period. In patients who experienced LF, we found a significantly lower D90% and V100% when evaluated several years later, suggesting that the quality of the primary implant was poor in these patients. To determine whether prostate cancer patients who did not relapse after pPPI have similar dosimetric observations several years later would require a cohort of patients followed over a long period and include negative biopsies.

Given this, the assessment of the dosimetry several years after pPPI remains a technical challenge. Most of the patients who were referred to the UCSF for LF after pPPI had been treated in other institutions, and it was often impossible to have any dosimetric data regarding the primary plan. In this pragmatic study, we have proposed a simple method to reconstruct the initial dose delivered with pPPI based on a pelvic MRI performed at t_f. Van Vulpen et al. attempted to correlate dose mapping with LF mapping inside the prostate in 14 patients previously treated with either external beam radiotherapy or pPPI [20]. The correlation between local recurrence on functional MRI and dosimetric plans suggested that some local relapses occurred in low-dose areas. The authors pointed out all of the variables that cloud this correlation.

The assessment of dosimetric plans when evaluated on CT scans performed 4 weeks after pPPI remains questionable. There is high inter-observer variability in prostate delineation and plan assessment [18]. Multi-parametric MRI performed at t_f has several advantages over a post-pPPI CT-scan. First, it allows the detection and mapping of a macroscopic local relapse inside the prostate while ruling out seminal vesicle and/or nodal involvement. Second, as the prostate shrunk over years after pPPI, the ultimate position of the seeds can be detected easily on MRI (punctiform absence of signal). Third, the contours of the prostate and its relationship with surrounding tissues are more accurate. Our expansion algorithm using the VCF makes it possible to infer post-implant dosimetry from an MRI scan performed several years after the implantation (at t_f) [13].

Salvage whole-gland treatments with surgery or brachytherapy for intra-prostatic failure are feasible with good oncological outcomes, but some patients may experience harmful late toxicity [5,7]. A focal salvage approach, if feasible, could decrease the rates of such sequelae [6].

In our present study, we found a strong correlation between microscopically recurrently-invaded sextants and low-dose areas. Chopra et al., like others, found that in 90% of patients with recurrent prostate cancer, the tumor recurs at the primary dominant intra- prostatic lesion [21–24]. Regarding microscopic involvement, the authors found that 83% of the patients had recurrent cancer in sextants with the involvement of ≥40% of core length on biopsy [23]. This is of particular interest in the context of focal salvage brachytherapy, as low-dose areas after pPPI might benefit from an additional dose of radiation with salvage brachytherapy without increasing the risk of toxicity.

Unsurprisingly, we found that the number of cold sextants was significantly greater than the number of pathologically invaded sextants, suggesting that sextant-biopsies alone are inaccurate for mapping recurrences and could miss micrometastatic disease.

References

1. Cooperberg MR, Broering JM, Carroll PR. Time trends and local variation in primary treatment of localized prostate cancer. J Clin Oncol. 2010; 28:1117–23. [PubMed: 20124165]
2. Blasko JC, Grimm PD, Sylvester JE, Badiozamani KR, Hoak D, Cavanagh W. Palladium-103 brachytherapy for prostate carcinoma. Int J Radiat Oncol Biol Phys. 2000; 46:839–50. [PubMed: 10705004]
3. Zelefsky MJ, Kuban DA, Levy LB, et al. Multi-institutional analysis of long-term outcome for stages T1–T2 prostate cancer treated with permanent seed implantation. Int J Radiat Oncol Biol Phys. 2007; 67:327–33. [PubMed: 17084558]
4. Pound CR, Brawer MK, Partin AW. Evaluation and treatment of men with biochemical prostate-specific antigen recurrence following definitive therapy for clinically localized prostate cancer. Rev Urol. 2001; 3:72–84. [PubMed: 16985694]
5. Burri RJ, Stone NN, Unger P, Stock RG. Long-term outcome and toxicity of salvage brachytherapy for local failure after initial radiotherapy for prostate cancer. Int J Radiat Oncol Biol Phys. 2010; 77:1338–44. [PubMed: 20138442]
6. Hsu CC, Hsu H, Pickett B, et al. Feasibility of MR imaging/MR spectroscopy-planned focal partial salvage permanent prostate implant (PPI) for localized recurrence after initial PPI for prostate cancer. Int J Radiat Oncol Biol Phys. 2013; 85:370–7. [PubMed: 22672747]
7. Moman MR, van der Poel HG, Battermann JJ, Moerland MA, van Vulpen M. Treatment outcome and toxicity after salvage 125-I implantation for prostate cancer recurrences after primary 125-I implantation and external beam radiotherapy. Brachytherapy. 2010; 9:119–25. [PubMed: 19850536]
8. Nguyen PL, Chen MH, D'Amico AV, et al. Magnetic resonance image-guided salvage brachytherapy after radiation in select men who initially presented with favorable-risk prostate cancer: a prospective phase 2 study. Cancer. 2007; 110:1485–92. [PubMed: 17701957]
9. Nyholm T, Jonsson J, Soderstrom K, et al. Variability in prostate and seminal vesicle delineations defined on magnetic resonance images, a multi-observer, - center and -sequence study. Radiat Oncol. 2013; 8:126. [PubMed: 23706145]
10. Debois M, Oyen R, Maes F, et al. The contribution of magnetic resonance imaging to the three-dimensional treatment planning of localized prostate cancer. Int J Radiat Oncol Biol Phys. 1999; 45:857–65. [PubMed: 10571190]

11. Rasch C, Barillot I, Remeijer P, Touw A, van Herk M, Lebesque JV. Definition of the prostate in CT and MRI: a multi-observer study. Int J Radiat Oncol Biol Phys. 1999; 43:57–66. [PubMed: 9989514]
12. Smith WL, Lewis C, Bauman G, et al. Prostate volume contouring: a 3D analysis of segmentation using 3DTRUS, CT, and MR. Int J Radiat Oncol Biol Phys. 2007; 67:1238–47. [PubMed: 17336224]
13. Pickett B, Chen J, Yu N, Weinberg V, Kurhanewicz J, Cory K, Pouliot J, Cunha JA, Shinohara K, Roach M III. MRI based dosimetric reconstruction with volumetric deformation for patients with recurrent prostate cancer under evaluation for salvage brachytherapy (SBT). American Society of Therapeutic Radiology Oncology Annual Meeting, Oral Presentation. Int J Rad Oncol Biol Phys. 2009:S332–3.
14. Grimm P, Billiet I, Bostwick D, et al. Comparative analysis of prostate-specific antigen free survival outcomes for patients with low, intermediate and high risk prostate cancer treatment by radical therapy. Results from the Prostate Cancer Results Study Group. BJU Int. 2012; 109:22–9. [PubMed: 22239226]
15. Stone NN, Stock RG, White I, Unger P. Patterns of local failure following prostate brachytherapy. J Urol. 2007; 177:1759–63. discussion 1763–54. [PubMed: 17437808]
16. Coen JJ, Zietman AL, Thakral H, Shipley WU. Radical radiation for localized prostate cancer: local persistence of disease results in a late wave of metastases. J Clin Oncol. 2002; 20:3199–205. [PubMed: 12149291]
17. Stock RG, Stone NN, Tabert A, Iannuzzi C, DeWyngaert JK. A dose–response study for I-125 prostate implants. Int J Radiat Oncol Biol Phys. 1998; 41:101–8. [PubMed: 9588923]
18. De Brabandere M, Hoskin P, Haustermans K, Van den Heuvel F, Siebert FA. Prostate post-implant dosimetry: interobserver variability in seed localisation, contouring and fusion. Radiother Oncol. 2012; 104:192–8. [PubMed: 22857857]
19. Stock RG, Stone NN, Dahlal M, Lo YC. What is the optimal dose for 125I prostate implants? A dose-response analysis of biochemical control, posttreatment prostate biopsies, and long-term urinary symptoms. Brachytherapy. 2002; 1:83–9. [PubMed: 15062175]
20. van Vulpen M, van den Berg CA, Moman MR, van der Heide UA. Difficulties and potential of correlating local recurrences in prostate cancer with the delivered local dose. Radiother Oncol. 2009; 93:180–4. [PubMed: 19700213]
21. Arrayeh E, Westphalen AC, Kurhanewicz J, et al. Does local recurrence of prostate cancer after radiation therapy occur at the site of primary tumor? Results of a longitudinal MRI and MRSI study. Int J Radiat Oncol Biol Phys. 2012; 82:e787–793. [PubMed: 22331003]
22. Cellini N, Morganti AG, Mattiucci GC, et al. Analysis of intraprostatic failures in patients treated with hormonal therapy and radiotherapy: implications for conformal therapy planning. Int J Radiat Oncol Biol Phys. 2002; 53:595–9. [PubMed: 12062602]
23. Chopra S, Toi A, Taback N, et al. Pathological predictors for site of local recurrence after radiotherapy for prostate cancer. Int J Radiat Oncol Biol Phys. 2012; 82:e441–448. [PubMed: 22284038]
24. Pucar D, Hricak H, Shukla-Dave A, et al. Clinically significant prostate cancer local recurrence after radiation therapy occurs at the site of primary tumor: magnetic resonance imaging and step-section pathology evidence. Int J Radiat Oncol Biol Phys. 2007; 69:62–9. [PubMed: 17707266]

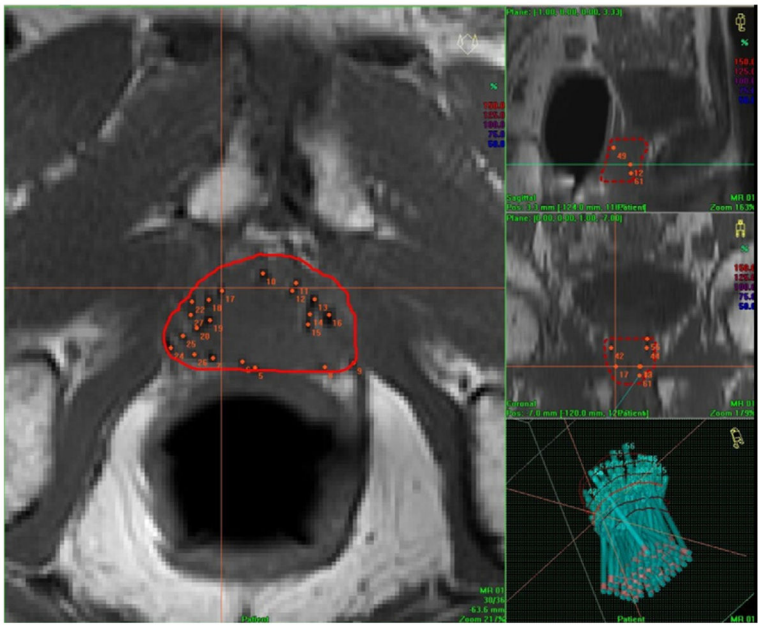

Fig. 1.

T1-weighted axial, sagittal, and coronal views of a patient with locally relapsing prostate cancer after primary prostate permanent implant with I^{125}. The prostate is outlined in red on each slice. The central position of each seed is defined by pinpointing each seed with the tip of an HDR catheter in the planning system.

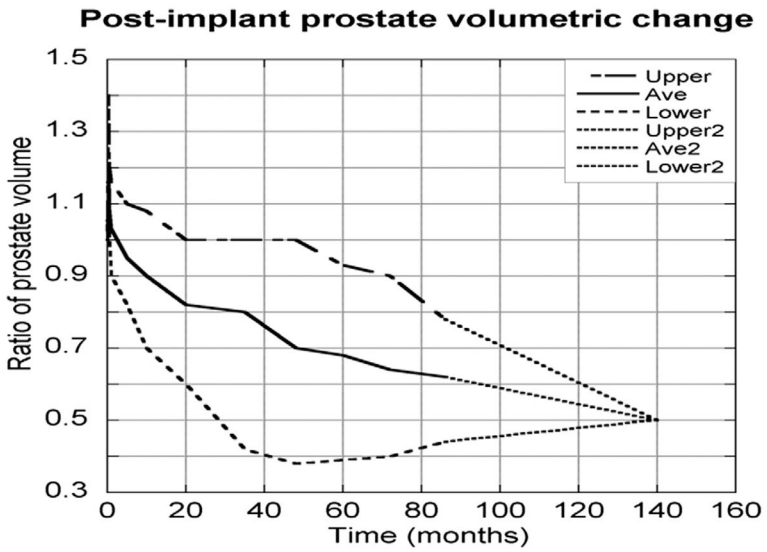

Fig. 2.

Graph representing the decrease in prostate size on MR imaging over time (n = 79 patients representing 420 MR scans).

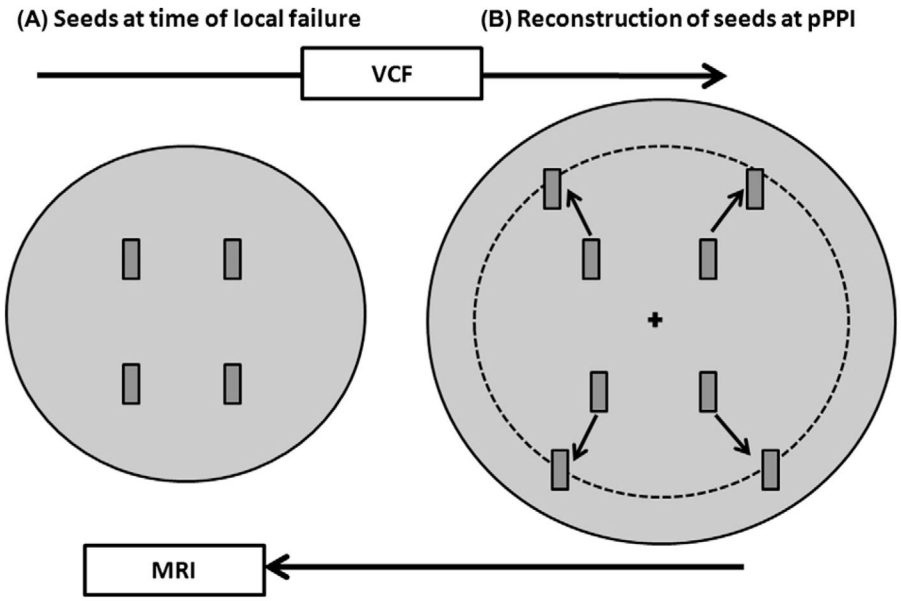

Fig. 3.
Reconstruction of initial prostate volume and seed positions.

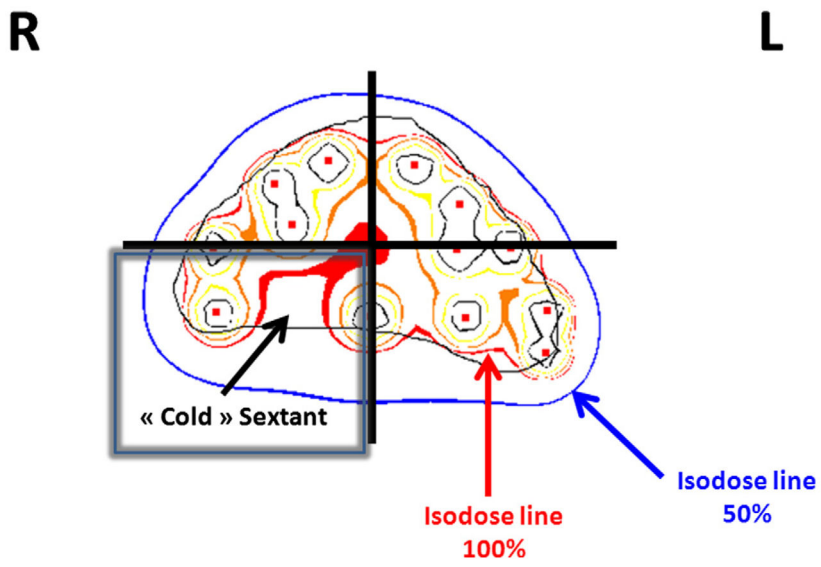

Fig. 4.

Correlation between cold spots on dosimetry and pathologically invaded sextants on TRUS-biopsy.

Table 1

Characteristics of pPPI and local failure (n = 24).

Characteristics *(n = 24)*	***N* (%)**
Baseline (pPPI)	
Nb of positive sextant/total nb of sextants (n = 15)	37/90
Gleason score (n = 21)	
≤3 + 3	16 (76.2)
3 + 4	4 (19.0)
4 + 3	1 (4.8)
Type of radioelement	
$Iodine^{125}$	20 (83.3)
$Palladium^{103}$	4 (16.7)
PPI as a boost	7 (29.2)
Mean activity per seed (mCi)	
Iodine ^{125}	0.384 [0.303–0.432]
Palladium ^{103}	1.2 [1.0–1.6]
Dose prescription	
Monotherapy – mean [range]	145 Gy [144–160]
Boost – mean [range]	103 Gy [100–108]
Mean number of seeds implanted [range]	84 [49–146]
Local failure	
Nb of positive sextants	36/144
Nb of patients with path+ SV	4 (16.7)
Gleason score	
Not assessable post-radiation	7 (29.2)
3 + 3	10 (41.6)
3 + 4	2 (8.3)
4 + 3	1 (4.2)
4 + 4	2 (8.3)
3 + 5	1 (4.2)
4 + 5	1 (4.2)
Mean prostate volume on MRI [range]	40.8 cm^3 [21.8–71.8]
Mean magnification factor [range]	0.66 [0.50–0.83]
Mean interval between pPPI and LF [range]	72.3 months [18–145]
Mean number of seeds found on MRI [range]	83 [49–143]

Table 2

Comparison of treatment characteristics at baseline and reconstituted at failure (n = 24).

Variable	*N*	Mean	SD	p50	Min.	Max.	*p*-Value
Dose prescribed at t_0 (Gy)	23	132.3	19.96	144	100	160	**0.001**
D90% (t_f)	23	95.265	30.78	93	39	147	
D90% (Gy)							**0.001**
t_0	14	145.2	19.16	150	100	167.5	
t_f	14	85.28	27.36	82	39	139	
V100% (%)							**0.0006**
t_0	20	91.55	7.95	93.55	70	100	
t_f	20	73.1	13.76	69	55	98	